PAPER

Evaluation of the Northern Gulf of Mexico Littoral Initiative Model Based on the Observed Temperature and Salinity in the Mississippi Bight

AUTHORS

Nadya Vinogradova
Sergey Vinogradov
Atmospheric
and Environmental Research, Inc.

Dmitri Nechaev
Vladimir Kamenkovich
The University of Southern Mississippi

Alan F. Blumberg
Stevens Institute of Technology

Quamrul Ahsan
Honghai Li
HydroQual, Inc

ABSTRACT

Temperature and salinity measurements from the Northern Gulf of Mexico Littoral Initiative (NGLI) survey during August 30 - September 14, 2000 reveal a high level of temporal and spatial variability in the Mississippi Bight. To support scientific studies using a numerical model, a three-dimensional hydrodynamic Estuarine and Coastal Ocean Model (ECOM) is implemented in the Mississippi Bight. The ECOM is run with realistic topography, stratification and meteorological forcing to hindcast circulation on a shallow and highly variable shelf of the Mississippi Bight. The results of the model are compared with observation to evaluate the ECOM performance on different temporal scales. Based on the area oceanography and data availability, three temporal scales are chosen for model/data comparison: fine scale (less than an hour), diurnal, and large scale (a two-week period). Limitations of the ECOM application on each scale are discussed. The model is capable to reproduce observed water masses, describe spatial distribution of water properties, and simulate areas with high horizontal gradient such as freshwater plumes. However, delayed response to meteorological forcing, overestimated mixing rates and uncertainties in computation of river discharges result in statistically significant bias in the simulations. Along with traditional linear correlations from all observational points and spectral analysis over the diurnal cycle, a new technique of model validation is introduced. The technique is a new application of an existing variational interpolation method. Detailed description of the method and numerical procedure allow one to apply this technique to any oceanographic data with prescribed data variances for model/data comparison.

INTRODUCTION

The Mississippi Bight shelf is an area of considerable interest to marine commerce, human recreation, oil and gas exploration and development. In addition, commercial fishing activity is an integral part of the economy of the region. Geologically, the Mississippi Bight shelf is wide due to comparative tectonic stability; the coastal plain is broad and of low relief, allowing abundant and extensive estuaries to intrude inland. As a typical Gulf of Mexico estuary, Mississippi Sound is a bar-built system with a flat topography (Schroeder and Wiseman, 1999). It stretches for approximately 130 km along Louisiana, Mississippi and Alabama coastlines and is separated from the Northern Gulf of Mexico by sandy barrier islands (Figure 1) at a distance of about 15 km from the mainland (Kjerfve, 1983). Mississippi Sound receives large discharges of fresh water from the major rivers of Mississippi and Mobile as well as many minor rivers and numerous bayous. The freshwater influx data suggests that buoyancy driven currents play an important role in the estuary circulation. Mean depth of the Mississippi Sound is 3 m (Kjerfve, 1983), which indicates that wind is another mechanism that dominates in the estuary. In addition, multiple connections to the Northern Gulf of Mexico through a number of passes between barrier islands allow important interaction between the estuarine and the Gulf of Mexico waters. These features present a unique circulation pattern and control the long-term dynamics.

To describe complex features of the Mississippi Bight circulation, an extensive set of observations is required. However, measurements used in the early studies were limited. For example, Kelly (1991) studied circulation and hydrography of the Mississippi Bight using five current meter moorings and twelve CTD stations, while the study of Brooks (1984) was based on the observations from four moorings and eight CTD stations. Significant progress was achieved in 1999 – 2001, when a series of oceanographic surveys were conducted, collecting high-resolution data in the Mississippi Bight area. More than a thousand CTD stations were sampled over a two-year period, covering the area of more than 30,000 km^2 (Vinogradov et al., 2004). These surveys were conducted in support of the Northern Gulf of Mexico Littoral Initiative (NGLI) program. The NGLI system was established as both an operational Navy product and a research tool used to benefit Gulf Coast economies and the marine environment (Asper et al., 2001). Besides observations, another constituent of the NGLI program is a modeling system. Prediction of the coastal ocean circulation is one of the most challenging issues in numerical modeling.

FIGURE 1

Map of the Mississippi Bight region. White circles indicate the CTD sampling locations of the R/V Pelican hydrographic survey during August 30 – September 14, 2000. Black dots represent the ECOM horizontal curvilinear grid.

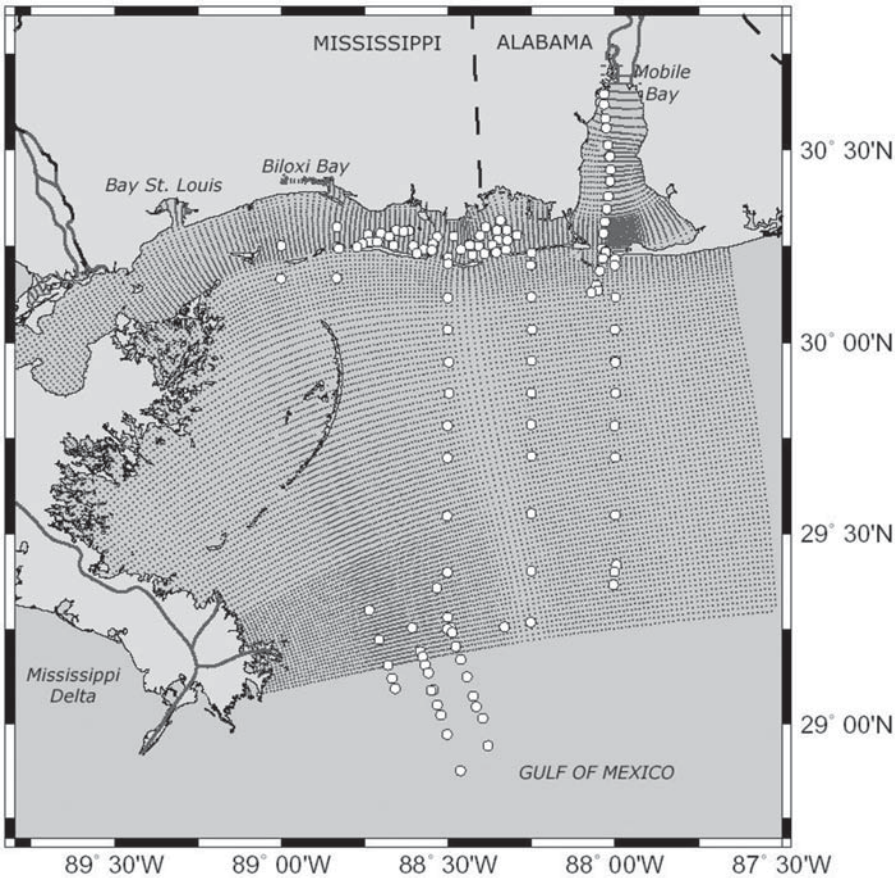

Circulation on the shelf is influenced by a variety of processes, such as winds, topography, complex coastline, shelf wave propagation, storm surges and many others (Allen et al., 1995; Chen and Beardsley, 2002; Klink, 1995; Fong and Geyer, 2001). In order to ensure that a numerical model is capable of reproducing and predicting a coastal circulation, thorough validation efforts are required. It is usually done through comparison of the model with the data, which leads to model improvement. The Estuarine and Coastal Ocean Model (ECOM) is one of the NGLI models. It is designed by HydroQual, Inc. The ECOM is a three-dimensional, time-dependent, sigma-coordinate model that computes circulation and mixing patterns of the coastal ocean. ECOM proved to be a useful tool for investigating the mechanisms of the upwelling circulation along the Oregon Continental Shelf (Allen et al., 1995) as well as wind and tide forced processes in Chesapeake Bay (Blumberg et al., 1990) and Georges Bank (Chen et al., 1995). The NGLI experiment provides a unique opportunity for model/data comparison in the Mississippi Bight.

The primary goal of this paper is to evaluate the capability of the ECOM to describe hydrodynamics in the Mississippi Bight shelf on different temporal scales. Evaluation of the model on different scales is critical as it represents applicability of the model to different oceanic processes. For example, the model's ability to reproduce processes on a daily scale is important for studying tidal dynamics, whereas in climatological and planetary studies a large-scale model performance is crucial. The model skill assessment is carried out through comparison of the ECOM hydrodynamics with the observed temperature and salinity. ECOM simulations correspond to one of the NGLI oceanographic surveys, collected during August 30 - September 14, 2000. When the simulated values are compared with temporally and spatially matched data, the model performance on small scales can be evaluated. Analysis of time series stations (25-hours anchor stations) allows one to compare the model with the data on the daily scale. The largest temporal scale, on which the ECOM performance is analyzed, is the period of the survey, i.e. two weeks. Unfortunately, the lack of simulations corresponding to other NGLI surveys does not allow one to consider larger temporal scales, such as seasonal and inter-annual scales, necessary for a thorough model validation. However, as mentioned earlier, for a highly variable shelf such as Mississippi Bight, a two-week period is a sufficient time to establish the circulation pattern. Consequently, a model/data comparison within this period does provide the information about the ability of the ECOM to identify major physical processes on the Mississippi Bight.

The next section describes the oceanographic observations collected in the study area, followed by the description of the model and the methods used to compare the simulations with the measurements. The results and discussion provide information on the advantages and limitation of the ECOM implementation in the area.

Oceanographic Observations

During August 30 - September 14, 2000, a 15-day survey was conducted in support of the NGLI program. The fieldwork was carried out on the R/V *Pelican*. A total of 178 full depth discrete conductivity – temperature – depth (CTD) stations were employed as illustrated in Figure 1. The hydrographic data went through a quality control procedure and oceanographic analysis (Vinogradov et al., 2004). The corresponding T-S diagram (Figure 2a) clearly demonstrates the existence of four water masses. There are hot and very low-salinity coastal waters, hot and low-salinity surface waters, warm and salty mid-water column (intermediate) and cool and

saline deep waters. The characteristics of the water masses are given in Table 1. The waters in the mixed layer are well stirred, which is demonstrated by the horizontal portion of the T-S diagram (Figure 2a). The deep waters have the same salinity level, which corresponds to the vertical portion of the T-S diagram. The right corner of the T-S diagram illustrates mixing between the shallow estuarine and the deeper shelf waters. The splitting of the T-S diagram here represents two different mixed layers in the area. Both layers are characterized by hot temperature, ~29 °C at a depth of about 20 – 25m (Figure 2b). However, their salinities are different. One layer is located closer to the coast. It has lower salinity of about 32 ppt as a result of the close proximity to the river inflow. There is a different mixed layer further offshore. It is close to the shelf break and it has a higher salinity of about 36 ppt. The water with temperature ~29 °C and salinity 36 ppt is a typical water mass for the surface waters in the Gulf of Mexico, which as the observations show can be found as far onshore as the shelf break area.

FIGURE 2

(a) T-S diagram and (b) temperature and salinity vertical profiles from the CTD measurements collected as shown in Figure 1.

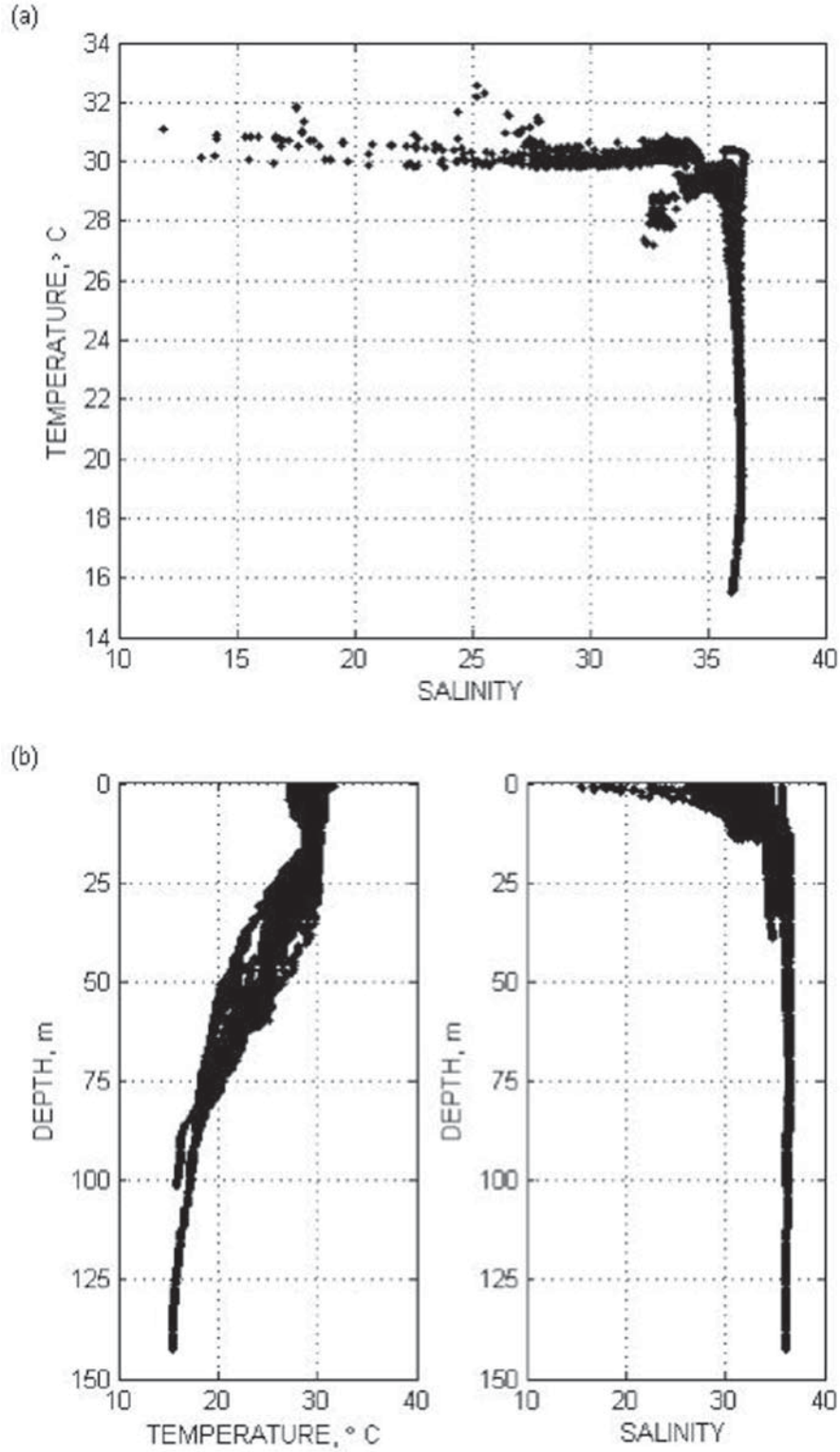

TABLE 1

Hydrographic features of the four water masses observed during August 30 - September 14, 2000.

Water mass	Temperature °C	Salinity	Depth m
Coastal	30	15 – 26	< 20
Surface	30	26 – 34	< 20
Intermediate	22 – 28	36 – 37	20 – 100
Deep	15 – 20	35	> 100

Vinogradov et al. (2004) made the analysis of temporal and spatial variability of the hydrographic data in this region. They examined temperature and salinity fields measured over a period of two years. The oceanographic analysis revealed a high level of spatial and temporal variability in the region, which has an important impact on the distribution of the physical properties in the water, such as heat, salt, oxygen, sound speed and others. The survey conducted during August 30 – September 14, 2000 revealed the smallest spatial and temporal variations during 1999 - 2000. Mean data variability over a two-week period was estimated as 1 °C for temperature and 2 ppt for salinity. It includes the overall standard deviation of the data from the mean field over the period of the survey. Compared to the winter months, when the variability in the data was about 3 °C for temperature and 8 ppt for salinity, the variability during the summer is small (Vinogradov et al., 2004).

Numerical Model and Experiment Design

The ECOM is a three-dimensional, time dependent, sigma coordinate, free surface model. The numerical model seeks a solution of an initial-boundary value problem in a specified domain. Governing equations are in the Eulerian frame of reference, in the flux-conservation form. The system consists of the conservation equations for momentum, heat, salt and mass. Equation of state completes the set of seven equations for seven quantities: temperature, salinity, density, pressure and three components of velocity. The model uses the hydrostatic and Boussinesq approximations. The small subgrid processes, such as horizontal and vertical mixing of momentum and scalars, are parameterized using the turbulence closure. The vertical mixing coefficients are computed using the Mellor-Yamada level 2.5 turbulence closure scheme (Mellor and Yamada, 1982). The horizontal mixing of the momentum and scalars is represented by the Laplacian terms. The horizontal diffusivity coefficients are mean-deformation-rate-dependent (Smagorinsky, 1963). This implies that the eddy coefficients are related to the simulated flow scales, rather than being constant. For this implementation, the background (constant) vertical mixing is 1×10^{-5} m^2/s. The constant value used in Smagorinsky's formula for horizontal mixing is 1×10^{-1} (non-dimensional). The ratio of viscosity to diffusivity (Prandtl number) is 1.0 both for horizontal and vertical mixing. The effect of rotation is introduced by the Coriolis parameter, which is computed using the beta-plane approximation.

The governing equations are formulated in the local orthogonal curvilinear coordinates in the horizontal and the bottom-following sigma coordinate in the vertical. The horizontal curvilinear system allows one to resolve a complex geometry of the Mississippi Bight coastline, featuring numerous bays, estuaries and bayous. The use of the sigma coordinate, which varies in proportion to depth, permits one to resolve the bottom boundary layer. It has been shown that such a coordinate system suits to modeling of the shallow coastal ocean better than the ordinary Cartesian coordinate system (Gerder, 1993). The horizontal grid used in this study is shown on Figure 1. The horizontal grid is non-uniform in space, with the resolution varying from 3 km to 100 m. The finest grid corresponds to the regions with the high gradients of water properties, such as the passes between the barrier islands, ship channels and the Mississippi River mouth. The 11 sigma levels in the vertical are evenly spaced. For a shallow region such as Mississippi Sound, where maximum depth is 10 m, the resolution exceeds 1 m in the vertical. In the deepest areas of the domain, close to the shelf break, the vertical resolution is about 7 – 10 m. A high-resolution model grid contains 165 x 121 x 11 grid cells.

The ECOM equations are discretized on an Arakawa C-grid, and are solved explicitly for the horizontal derivatives and implicitly for the vertical. The advection of salt and heat is handled using the Smolarkiewicz scheme (Smolarkiewicz and Grabowski, 1990), which corrects numerical diffusion better than other advective schemes. The model incorporates a mode splitting technique, solving the two-dimensional equations for the fast (external) processes, and the three-dimensional equations for the slower (internal) processes. For this study, the internal step is 60 s and the external step is 6 s. The model is integrated from the state of 00:00 UT, July 1, 2000 for 3 months, which covers the sampling period of August 30 – September 14, 2000.

There are two types of the lateral boundary conditions used in this model configuration—coastal and open ocean boundaries (see Figure 1). At the coastal wall the normal component of velocity and the normal gradients of temperature and salinity are zero. Along the open boundaries, the sea surface elevation, temperature and salinity fields are specified. The open boundary conditions are time-variable. The temporal increment is one hour for the surface elevation and two days for the temperature and salinity fields. The elevation boundary conditions are derived from the Oregon State University tidal model (Blumberg et al., 2002). The tidal forcing at the open boundary is specified using the inverse Reid and Bodine boundary condition, which allows longwave energy, such as tides, to enter and radiate out of the model domain. The time-varying temperature and salinity boundary conditions are specified at six depths in the vertical. The temperature and salinity are derived using the Modular Ocean Data Assimilation System, MODAS (Fox et al., 2001), provided by the Naval Oceanographic Office (NAVOCEANO).

The boundary conditions in the vertical are the conditions at the free surface and the bottom of the basin. The surface boundary conditions are the net ocean heat flux, the evaporation-precipitation fresh water surface flux, and the wind stress. The surface conditions are computed from the meteorological parameters, such as wind speed and direction, air temperature and humidity, provided by the Coupled Ocean Atmospheric Mesoscale Prediction System, COAMPS (Hodur, 1997). The surface conditions are time-variable as well and have a one-hour increment. On the lower boundary, there is no flow normal to the bottom of the basin and the fluxes of heat and salt are zero. The bottom frictional stress is determined from the logarithmic law of the wall (HydroQual, 2002). The bottom friction coefficient is set to 2.5×10^{-2}; the bottom roughness is 3×10^{-3} m.

The freshwater discharge is specified at the 26 grid cells, corresponding to the location of the Mississippi River, East and West Pearl River, Biloxi River, Wolf River, East and West Pascagoula River, Mobile River, and the other smaller rivers in the area. The ECOM freshwater sources, such as discharge flow, temperature and salinity of the flow, are specified daily, using the USGS measurements from the river monitoring gauges.

Model Evaluation Methods

The primary goal of this paper is to evaluate the ECOM hydrodynamics by comparison of simulated fields with ocean observations. In particular, the performance of the model on different temporal scales is of greatest interest. For a fine scale comparison, the ECOM results are matched with the observations in time and space. The model high-resolution horizontal grid allows matching the

station locations with high accuracy (Figure 1). Simulated fields have one-hour temporal resolution. Consequently, in time, the simulated and observed data are matched within a 30-minute interval. For example, 21:23 sampling time corresponds to the 21:00 model time, whereas 21:43 sampling time corresponds to 22:00 model time. Physical processes that have temporal scales smaller than a 30-minute interval are ignored in the current consideration. To match the model and the data vertically, the observations are interpolated onto the model depths using a cubic spline interpolation. The ECOM depths are determined using the computed sea surface elevation and the model bathymetry. It is worth noting that for certain stations there was a difference between the model bottom topography and the actual depth of the stations. Ahsan et al. (2002) showed that the model is extremely sensitive to the bathymetry. Its contribution to variances in model salinity might be as high as 76% and as high as 88% in temperature. To exclude the possibility of high model errors due to the bottom topography, the stations with large discrepancies between modeled and observed bathymetry are disregarded. About 10% of model/data comparisons are discarded due to bathymetric mismatches.

During this survey there were several stations at which the data were collected every hour over one day. The comparison of the time-series measurements with the corresponding simulations provides the analysis of the model performance on a daily scale. The analysis of a time series is usually done in a frequency domain, using a spectral analysis. The amplitudes, X_k, are computed using the fast Fourier transform algorithm (Frigo and Johnson, 1998). To avoid the aliasing of the spectra, the Fourier coefficients are computed for the frequencies lower than the Nyquist frequency,

$f_N = \frac{1}{2\Delta t}$. For the sampling interval

$\Delta t =$ 1 hour, the Nyquist frequency is

$f_N = 0.5$ hr^{-1}. The spectrum is computed as

$$S_k = |X_k|^2 = \frac{X_k^* \cdot X_k}{N} \qquad (1)$$

where X_k^* is the complex conjugate of X_k; $N = 26$ is a number of the data points in a time series station; and $k = 1 \ldots N/2$, since there are only $N/2$ meaningful Fourier coefficients for a discrete time series of N data points (Teng, 2003).

As mentioned above, the largest temporal scale of model/data comparison here is two weeks. For a large-scale analysis, simulations are temporally averaged over a two-week period, corresponding to the period of the survey. At the same time, observations were made only once at each station, not during a two-week period. To obtain a mean state of the ocean over two weeks having a single set of measurements, a variational interpolation technique is designed. The basic premise of the variational interpolation is to determine an optimal estimation of an oceanographic field approximating the data while exhibiting only small spatial variations. The variational interpolation can be considered as an application of Gauss–Markov theorem (McIntosh, 1990). The theorem determines the optimal estimate of the field of interest, which is unbiased, is linear in the data, and has the minimum variance, given prior the expectation value and covariance of both the field and the data. Specifically, an optimal estimation has to meet the following criteria: (1) the field is determined on a regular model grid rather than on a irregular observation net; (2) values of the field are consistent with the observations in the data locations; (3) the field is smooth; (4) data variability is taken into account; and (5) the field is dependent on the bottom topography and the coastline geometry. The last criterion is useful in the areas of a large bottom gradient, such as shelf break and barrier islands. The cross-isobathic variations across the shelf tend to be larger compared to the along-shelf variations. In the vicinity of the barrier islands, the circulation differs significantly on both sides of the island. The mathematical details and a numerical procedure of the optimal field derivation are shown in Appendix A.

One of the advantages of the variational interpolation is that, in addition to the optimal field, it allows one to compute the posterior error of the optimal estimator. In other words, one can determine the result reliability and see where the error of the method is large. The limits depend on the process of interest. In this paper, an optimal field estimates a biweekly mean state of the ocean. Therefore, the interpolation error includes the data variability over a two-week period. Based on that, the optimal field is considered reliable if its error does not exceed the standard deviation of the data error. The data error includes a mean variability of the measurements within the two weeks and the measurement error. As mentioned early, the mean variability of the data was estimated as 1° C for the temperature and 2 ppt for salinity during August 30 - September 14, 2000 (Vinogradov et al., 2004). The mathematical details of the error derivations are given in Appendix B.

Results

Model Performance on a Fine Temporal Scale

Figure 3 compares simulated and observed temperature and salinity at the surface, mid-water column and the bottom. The two sets have a positive linear relationship with a high degree of linear interrelationship (R^2 is 0.78 - 0.97). However, there is a significant bias in model temperature and salinity (see Table 2). The offset coefficients are negative for all depths, implying that the simulations are fresher and colder for ~80% - 90% of the sample points. The slope coefficients are close to 1.0. The higher values of the slope show that the rate of change in the simulations is generally higher compared to the observed rate of change. Figure 4 examines the regression residuals in order to check if the regression analysis is valid. The residual values are determined as a difference between the linear regression fit and the ECOM values at the three depths. The regression analysis is valid when the errors are independent and are normally distributed with the constant variances (Teng, 2003). As shown in Figure 3, there is no correlation between the independent variable, i.e. observations, and the regression residuals. At all depths, the histograms of the residuals are close to the symmetric (normal) distribution, slightly skewed right (posi-

tive skewness). The linear regression analysis is adequate here since there is no violation of the general error assumption.

To examine the overall discrepancies between the simulations and the data, the distribution of the model error is computed (Figure 5). The model error is defined as the difference between the matched simulations and the measurements (Chu et al., 2001). The model temperature errors are close to a Gaussian type. The mean temperature error is close to zero. The values of the standard deviation (STD) are 0.5 -1.2 °C. The slightly negative mean values of the model temperature errors show that the model underpredicts the temperature at all three layers. The model salinity errors reveal a bimodal distribution (non-Gaussian). The mean salinity error ranges from –2.6 ppt to –1.7 ppt and standard deviation varies from 1.7 ppt to 3.7 ppt. The first mode of model salinity error is around zero. The second mode is around –2 ppt, shifting the mean model salinity error to the left. The negative modes and a high percentage (96% - 97%) of the negative errors are indications that the model underestimated salinity.

Model Performance on a Daily Temporal Scale

The time series station, chosen for comparison with the simulated time series, was located in the ship channel at the Mobile Bay Pass during September 4 – 5, 2000 (see map in Figure 6). The depth at this location was 9.0 m. Figure 5 a-c examines the diurnal variability of the temperature and salinity at the surface (0.5 m), mid-water column (4.5. m) and the bottom (9m). Surface waters (Figure 6a) show a high degree of variability both in the model results and the observed data. The rate of change in the simulations is faster than the observed rate of change, which was already seen from Figure 3a and Table 1 for the surface water analysis. Bottom waters (Figure 6c) show a good model/data agreement, but with a negative temperature and salinity offset. Mid-water model temperature variations (Figure 6b) seem to be negatively correlated with the data. The mid-water model salinity values are smaller and change slower than the data. The same result of the model underestimating salinity is demonstrated on Figure 3b and was mentioned earlier in the text.

Estimation of the surface observed and simulated spectra is shown on Figure 6d. The dominant power peak for the surface temperature is at ~0.04 hr^{-1}, which is an inertial frequency in the Mississippi Bight shelf (Keen and Allen, 2000). The corresponding period is about 26 hours, which is very close to the period of the lunar diurnal tidal constituent O_1. The salinity spectra show a strong subinertial signal at frequency ~0.08 hr^{-1}, which corresponds to approximately a half-day period. The simulated spectra are very consistent with the observed ones. The ECOM shows the largest variability at the diurnal and semi-diurnal temporal scales, which is in agreement with the measurements. The spectra decrease with increasing frequency. For the temporal scales less than 6 - 7 hours (frequencies higher than 0.2 hr^{-1}), the signal is very weak, showing a small variability both in the model and in the data.

FIGURE 3

Simulated vs. observed temperature and salinity (a) at the surface, (b) at the mid-water depth and (c) at the bottom.

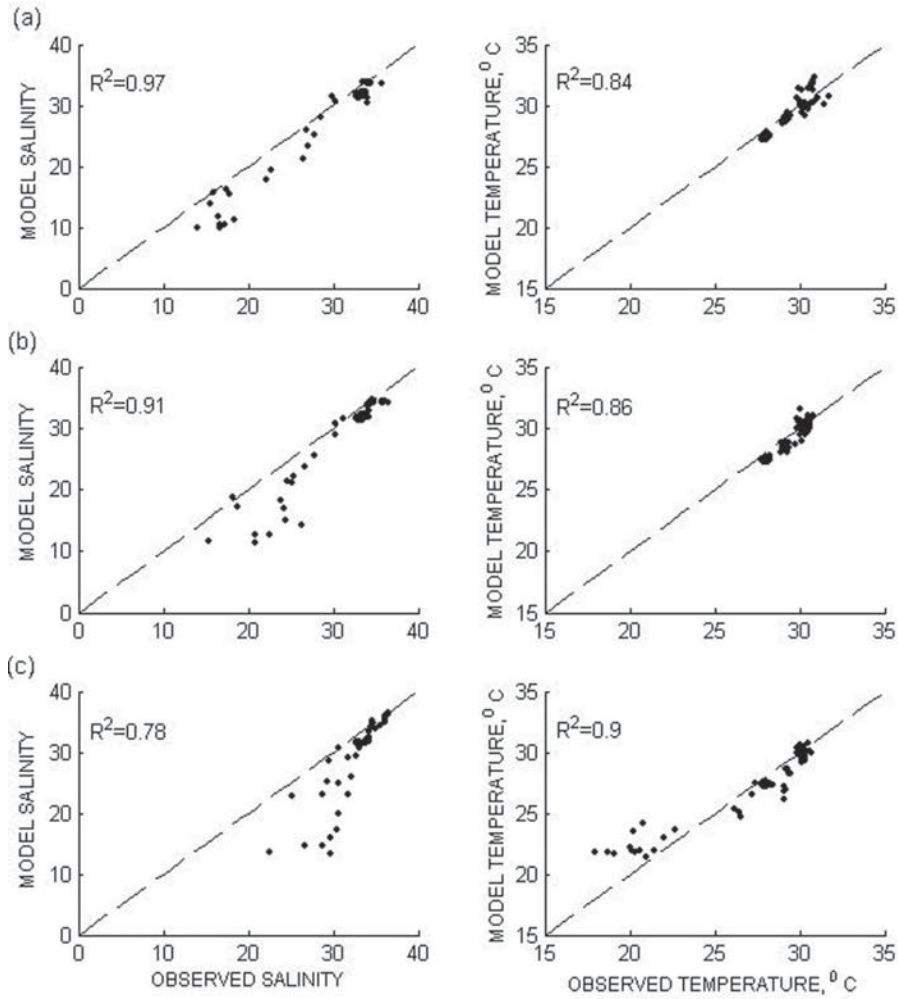

TABLE 2

Linear regression coefficients, computed for the simulated and observed temperature and salinity.

Water mass	R^2	Offset Coefficient	Slope Coefficient
Salinity			
Surface	0.97	-7.2	1.2
Mid-water	0.91	-11.9	1.3
Bottom	0.78	-13.8	1.9
Temperature			
Surface	0.84	-4.1	1.1
Mid-water	0.86	-5.2	1.2
Bottom	0.90	-6.6	0.8

FIGURE 4

Regression residual patterns and histograms of the temperature (right) and salinity (left) (a) at the surface, (b) at the mid-water depth and (c) at the bottom.

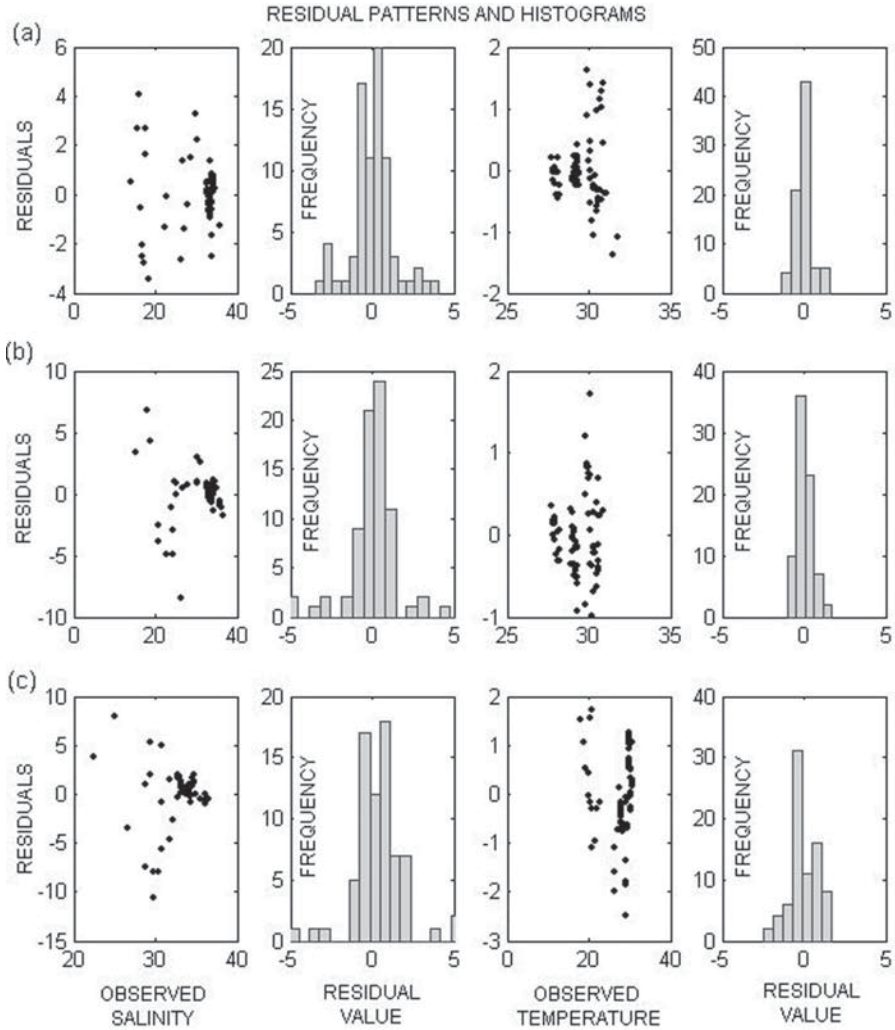

Model Performance on a Large Temporal Scale

The observations are variationally interpolated according to the technique described in Appendix A. Figures 7b and 8b show the optimal estimations of the biweekly mean surface salinity and temperature fields, respectively. Note that, in order to avoid data extrapolation, the optimal fields are determined only on the part of the ECOM grid, enclosed by the data locations (see Figure 1).

The horizontal salinity pattern (Figure 7b) reveals three distinctive regions. There is a high salinity offshore region (33 – 34 ppt), a less saline coastal area (30 – 32 ppt), and the region of minimum salinity (22 – 28 ppt) in the Mobile Bay. The relatively fresh-water outflow, spreading through the Mobile Bay Pass onto the shelf is clearly seen on Figure 7b. When the plume passes the barrier island (Dauphin Island, AL), it enters the shelf and propagates westward. The surface temperature (Figure 8b) is characterized by the hot coastal waters (30 – 30.5 °C), slightly cooler offshore water (29 – 29.5 °C), and the region of the minimum temperature west off Biloxi Bay (27 °C).

It is important to emphasize that the obtained estimations of the mean temperature and salinity are optimal. The fields meet all five criteria stated above (see Model Evaluation Methods section). The observations are interpolated from the original data locations onto the model fine resolution grid (condition 1). The values of the estimators are close to the observations in the data locations (condition 2) (not shown here). Both temperature and salinity estimators are smooth (condition 3) and are not spatially isotropic (condition 5). In particular, there is no correlation between the points on the different sides of the islands, though the points are geographically close. To examine the reliability of the estimators, the error analysis is performed (see Appendix B for the numerical procedure). As stated earlier, the technique is considered to give a reliable solution, when its error does not exceed the data error. Figures 7c and 8c show the standard deviations of the salinity and temperature interpolation errors, respectively (hereafter, referred as estimator error). Examination of these graphs shows that the estimator error does not exceed the prescribed data error, which is, as mentioned above, 1° C for temperature and 2 ppt for salinity for this survey. Therefore, the interpolation results are reliable over the basin shown in Figures 7 and 8.

The ECOM biweekly mean surface temperature and salinity are shown on Figure 7a and 8a, respectively. Both fields have zonal distribution. The surface temperature gradually decreases, whereas the surface salinity increases offshore. The observed freshwater plume in the Mobile Bay Pass (Figure 7b) is clearly identified in the simulations (Figure 7a). As previously seen from the analysis of the surface layer (Figure 3a), the simulations change faster, compared to the observations. The simulated freshwater plume is more pronounced compared to the observed one, which implies a faster propagation rate in simulations. In addition, overall simulations are slightly fresher and cooler as compared to the data.

To obtain a quantitative estimation of the model/data consistency, the difference between the two is divided by the error estimates. The relation gives a quantitative evaluation of the model/data discrepancy in terms of the standard deviation of the variational interpolation error (estimation error). If this ratio is less than one, then these two fields are consistent within one standard deviation of the method. The normalized salinity and temperature differences are presented in Figure 7d and 8d. The ratio does not exceed

FIGURE 5

Histograms of the model temperature (right) and salinity (left) errors (a) at the surface, (b) at the mid-water depth and (c) the bottom.

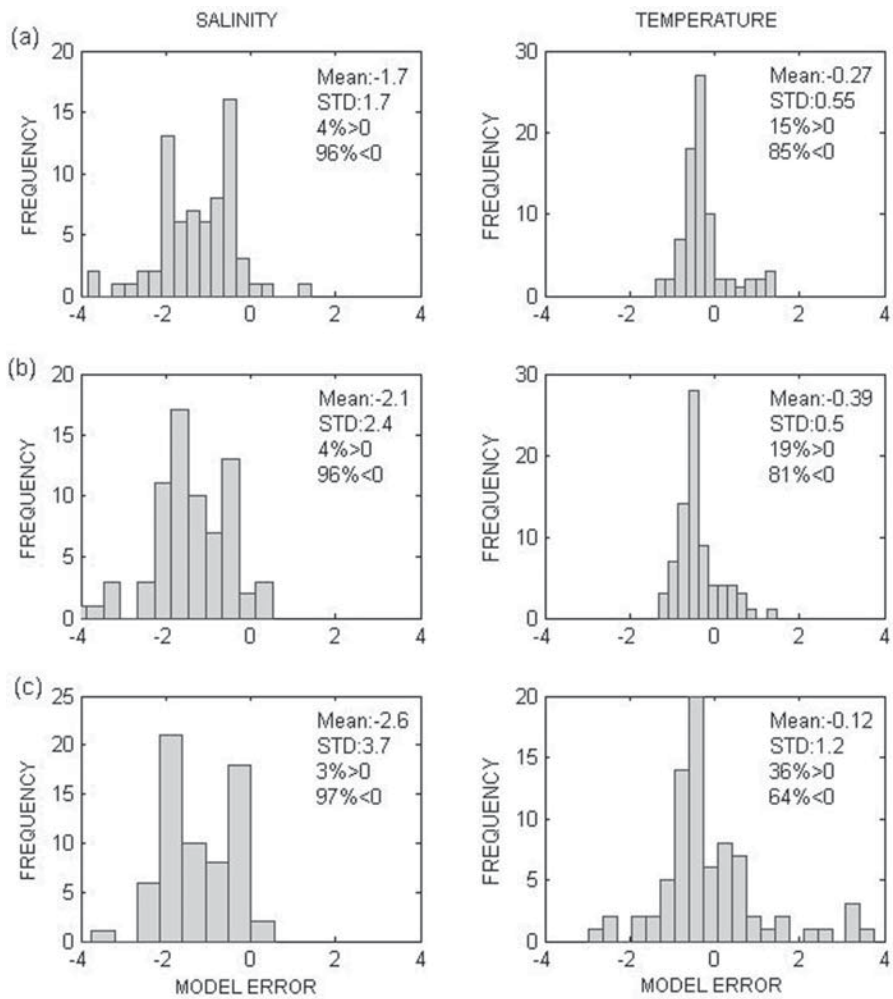

one standard deviation almost over the entire area, which implies the simulation and the data are consistent. The exceptions are several areas that are close to the coast. Specifically, in the northern Mobile Bay, the salinity ratio increases up to four standard deviations and temperature ratio increases up to two standard deviations. In addition, the temperature ratio grows in the west, where the minimum temperature was observed (Figure 8b).

Discussion

Observed temperature and salinity on the Mississippi Bight shelf reveal spatial and temporal variability during August 30 – September 14, 2000. Different water types are found near the coast and shelf break region, close to freshwater discharges and further offshore. In addition, an irregular coastline with many bayous and island passes adds to data spatial variability altering water mixing. Temporal variation in data is due to diurnal changes and shelf rapid response to meteorological forces such as wind. These measurements are used to validate one of the NGLI models, the ECOM. This type of analysis is necessary to support numerical studies in the Mississippi Bight and to justify model results for operation use in the area. Based on the region's oceanography, three temporal scales are chosen to analyze model performance. These are fine (less than an hour), diurnal, and large (two weeks) scales. As seen from observations, oceanic processes on these scales are important in shelf circulation. In the Mississippi Bight a strong tidal signal is close to lunar diurnal constituent, which is reflected in CTD data variability. In addition, rotating winds in the Mississippi Bight change their direction approximately every seven to ten days (Keen, 2002). Variations on the shelf are closely correlated with wind stress (Schroeder et al., 1987). Therefore, a two-week period is sufficient for circulation to develop in a shallow wind-driven shelf such as the Mississippi Bight. It would be desirable to see longer scales such as seasonal and inter-annual variations. However, only limited data were available. Nevertheless, three temporal scales are dominant within seasonal changes in the area. Therefore, analysis on these particular scales justifies model performance during a season in the shelf dynamics.

The ECOM skill assessment demonstrates the following strengths and weaknesses of the model. On a fine scale, about 80 – 90% of the simulations are linearly related with the observations. It includes shelf area and nearshore region that are far enough from river inputs. The remaining 10 – 20% of comparisons show a non-linear relation. These points represent surface and mixed layers, which are close to the coast with river inflows. In these points both temperature and salinity are underestimated by the model. There are two possible reasons for a non-linear relationship between the data and the simulation in these data points. The first reason is a difference between observed and simulated mixing rates. The observed mixing of the estuarine and shelf waters, which occurs just below the surface, is captured on the earlier stage as compared to the simulated one. In other words, the ECOM horizontal mixing is faster compared to the observed one. Simulated vertical mixing is also faster than the observed one. The faster simulated vertical mixing rates lead to smoother vertical gradients in the model profiles (not shown here), which result in the underestimated temperature and salinity. The second possible reason for the salinity bias is an uncertainty in specification of the river discharge information. It includes the estimation of the discharges in the un-gauged areas, the sensor

FIGURE 6

Observed and simulated salinity (left) and temperature (right) as functions of time at the Mobile Bay Pass station (a) at the surface, (b) at the mid-water depth and (c) at the bottom. (d) The surface spectra computed based on the simulations and measurements at the Mobile Bay Pass station.

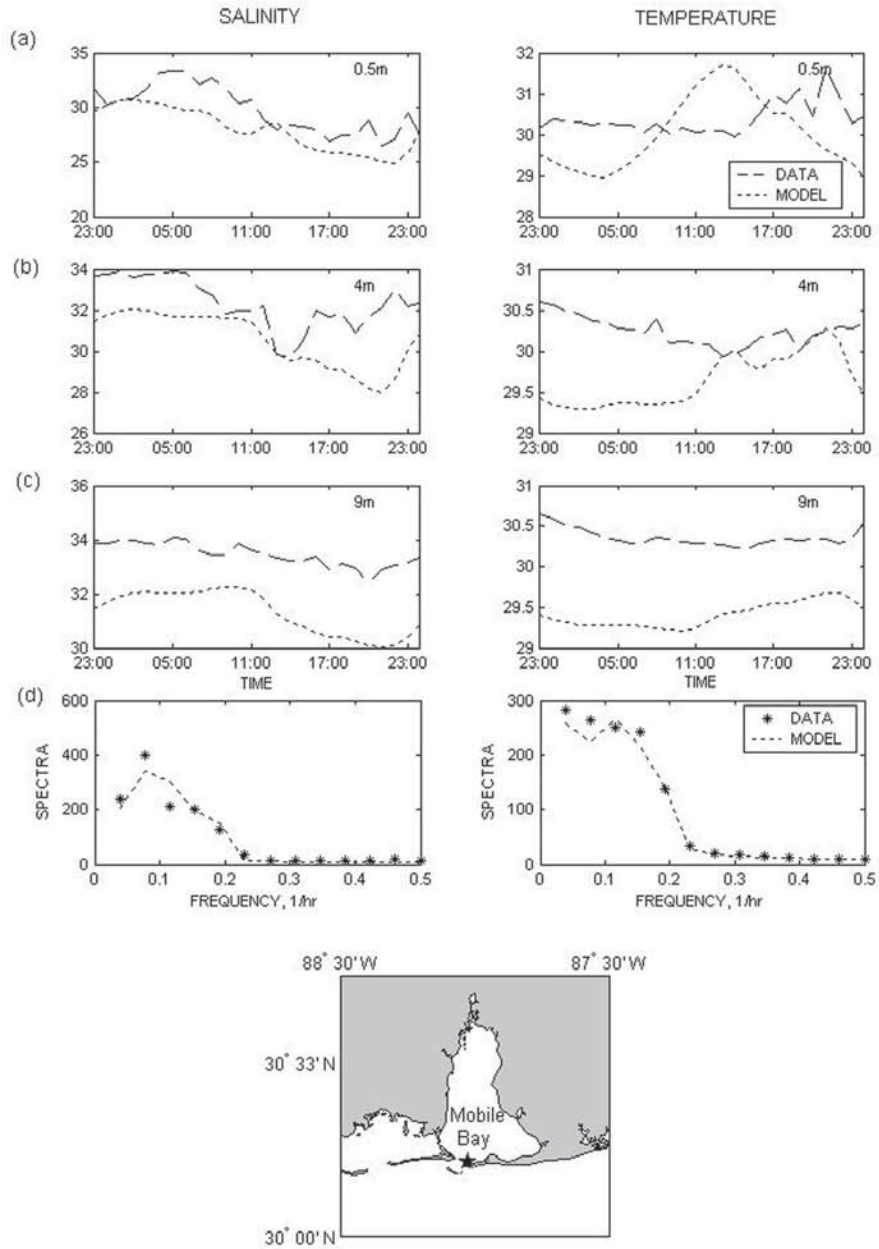

calibration and/or the specified inflow rates, which could be different from the actual rates. Therefore, on a fine temporal scale the ECOM performs reasonably well in 80% of the data points except in the regions that are close to the freshwater inflows and in the mixed layer of the water column.

The next dominant scale in the area is the diurnal cycle. The strong observed diurnal and semi-diurnal variability is well captured by the ECOM. The simulated and observed signals are in a good agreement, both having their energy peaks in the low frequencies (period of 26 and 13 hours). Both observed and simulated signals are gradually decreasing toward the higher frequencies (period less than 6 hours). A slight non-synchronization between the model and the data is likely due to different response to meteorological conditions. The northeastern wind prevailed during September 4 – 5, 2000, which is the day the time series data were collected. This resulted in the mixing between the water in the Mobile Bay Pass (station location) and warm and fresh coastal waters. The corresponding event in the model occurs with a 6 – 10 hours delay. Nevertheless, the general trend, observed in this area during a wind-induced mixing event, is reproduced by the ECOM.

The last temporal scale considered here is a two-week period. The observed integral large-scale horizontal patterns are seen in the temporally averaged simulations. Both qualitative and quantitative analyses show a good model/data consistency within the estimator error. Similar to the observations, the ECOM temperature and salinity increase offshore. In addition, the observed freshwater plume is also found in the simulations. When the simulated plume comes out to the Gulf through the Mobile Bay pass between the barrier islands, it is not destroyed by the horizontal mixing with the ambient water. The simulated plume enters the shelf area and propagates southwest similar to the observed plume path. The ability of the model to handle processes with high horizontal gradients is very important in studying the dynamics of the fronts. However, the cold front passage that was observed during CTD data collection is not captured by the ECOM. This, as mentioned earlier, is a result of the delayed response of the model to the meteorological forcing. In addition, there is an overall negative bias in the simulated mean characteristics due to the reasons mentioned above.

Conclusions

A quantifiable summary of the ECOM performance on different temporal scales is shown in Table 3. The main conclusion of this paper is that the ECOM is found to be useful to study coastal oceanography in the Mississippi Bight. It resolves general trends and dynamical features in the area, including determination of the main water masses and simulation of their spatial distribution in the area. In addition, areas of high horizontal gradients are well handled by the model, which is crucial in modeling shelf and slope regions of

FIGURE 7

Comparison of mean simulated and observed surface salinity. (a) biweekly mean model surface salinity; (b) biweekly mean surface salinity data, obtained using a variational interpolation method; (c) standard deviation of the variational interpolation error for surface salinity; and (d) the difference between a biweekly simulated and observed salinity fields divided by the error of the variational interpolation method.

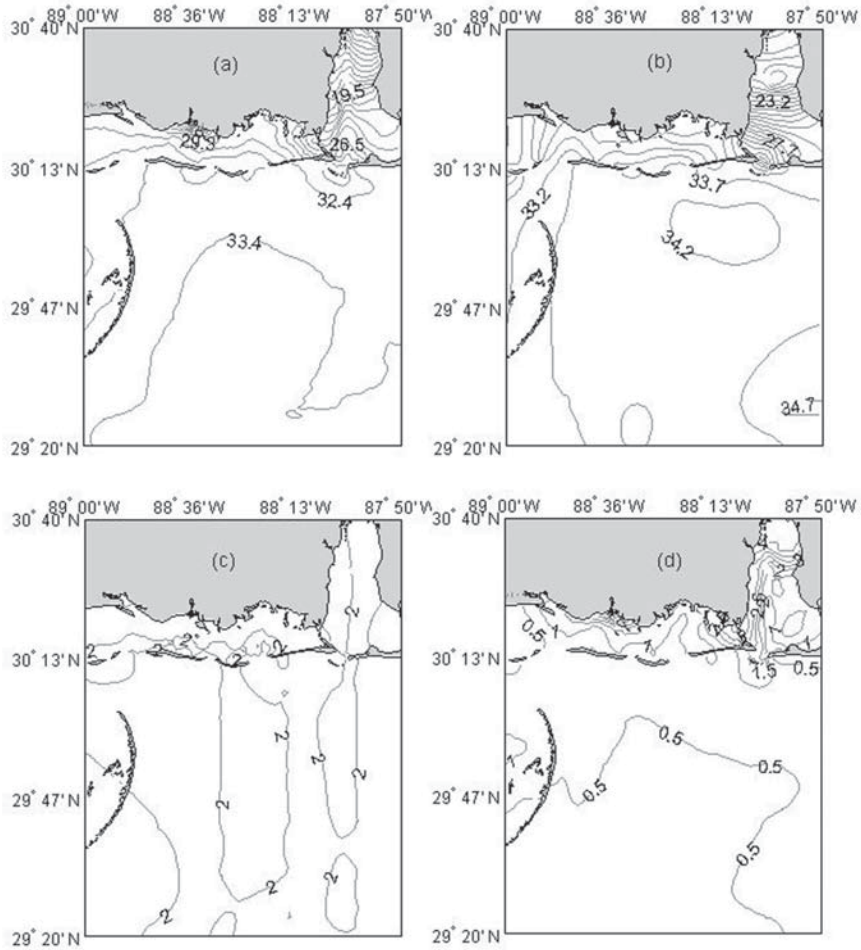

TABLE 3

Summary of the Model/Data comparison

Temporal Scale	Model Performance	
	Strength	Weakness
Fine scales (less than an hour)	· 80% of comparisons show strong positive linear correlation. · Surface layer and offshore areas are resolved by the model in 90% of comparisons	· 20% of comparisons show underestimated temperature and salinity. · Mixed layer and areas that are close to freshwater discharge are not resolved by the model in 60%-80% of comparisons.
Diurnal scale	· Both inertial (0.04 hr^{-1}) and sub-inertial (0.08 hr^{-1}) signals are captured by the model · General trend of response to meteorological forcing is similar	· Delayed response to meteorological forcing (about 6 hours)
Large scales (two weeks)	· Similar horizontal patterns are found in the model and the data · Model resolves areas of high gradients, such as freshwater plumes	· Model captures a rapid cold event with delay · Bias in the mean characteristics

the Mississippi Bight. However, the current performance of the ECOM is to be improved in order to be used operationally. In particular, the model biases in hydrographic field estimation and the model's delayed response to meteorological forces are major concerns in the current application of the ECOM.

Furthermore, the variational interpolation technique is reintroduced in this paper, which follows the approach described by McIntosh (1990). New application of an existing method is proved to be useful and effective as a new technique of model validation. The technique provides a reliable estimation of mean state of the ocean from observations. The method computes both the optimal field and its error, so one can control the limits of the solution acceptance. The numerical algorithm described in this paper is applied to one CTD survey of August 30 – September 14, 2000. Based on the data, a bi-weekly mean state of the ocean is estimated with an error of the solution less than the prescribed error. It is worth noting that this approach is not limited to a particular survey and can be applied to any data with prescribed data variances. This technique was successfully applied to observations collected during five other NGLI surveys (Vinogradov and Vinogradova, 2003). Prior to computation of the optimal fields, data variances for each survey were estimated by Vinogradov et al. (2004). The obtained mean temperature and salinity fields could be used to study seasonal climatology and inter-annual variability in the area. It could also be used as reference fields in regional numerical models to improve forecast systems in the Mississippi Bight.

Acknowledgements

The authors wish to thank John Blaha and Carl Szczechowski of NAVOCEANO for their support and assistance in data collecting and preprocessing. We benefited from valuable comments and thoughts on the draft manuscript by Mark Cobb (NRL) and discussion with Chung-Chu Teng (NDBC). We appreciate comments of two anonymous reviewers, whose suggestions helped us to improve the manuscript. This work was funded by CNMOC through N62306-01-D-BOO01-0002.

FIGURE 8

Comparison of a mean simulated and observed surface temperature. (a) biweekly mean model surface temperature; (b) biweekly mean surface temperature data, obtained using a variational interpolation method; (c) standard deviation of the variational interpolation error for surface temperature; and (d) the difference between biweekly simulated and observed temperature fields divided by the error of the variational interpolation method.

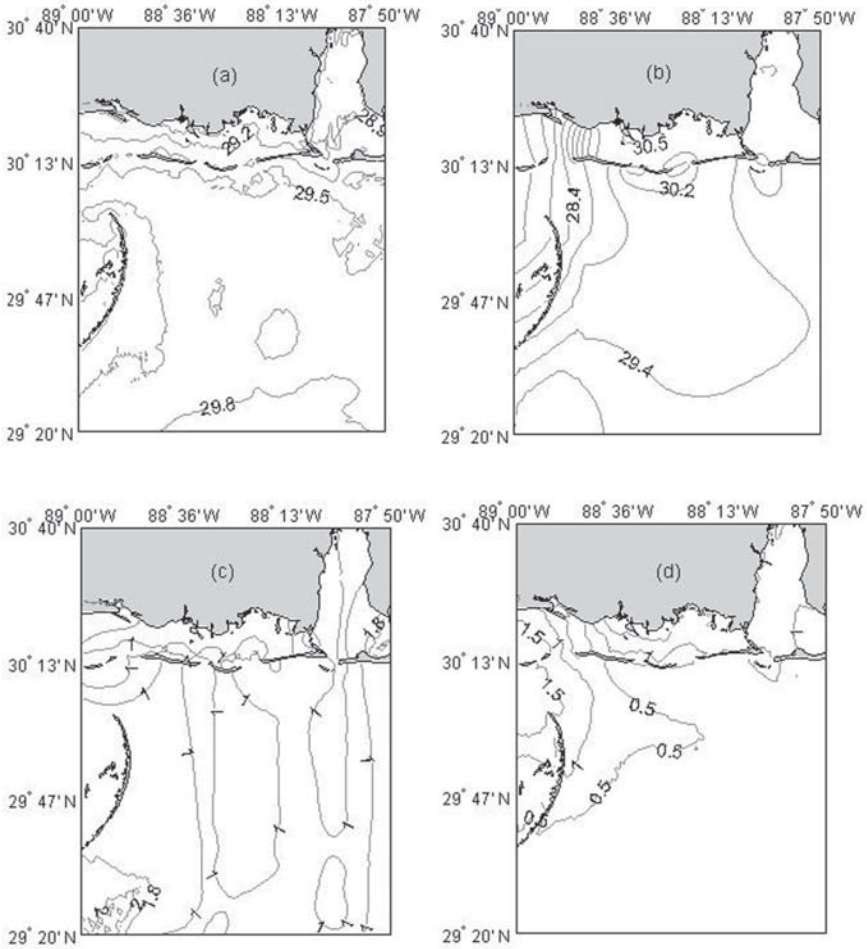

Appendix A

Variational interpolation technique

Consider the problem of estimating the field X (a mean temperature or salinity field over the observational period) from data values D, which measure the field X with some error. The Bayesian Maximum Likelihood approach allows one to build the optimal field X_{OPT}, which maximizes the conditional probability of the observed field X:

$$p(X \mid D) = \frac{p(D \mid X)\, p(X)}{p(D)} \xrightarrow[X]{} \mathbf{MAX}. \tag{A.1}$$

Maximization of the conditional probability (or minimization of the log-likelihood ratio, $-\log p(X \mid D)$) can be reduced to the minimization of the following cost function with respect to X:

$$J(X) = -\log p(D \mid X) - \log p(X) \xrightarrow[X]{} \mathbf{MIN}. \tag{A.2}$$

The term log $p(D)$ in (A.2) is not included since it does not depend on X. Definition of the conditional probability density $p(D \mid X)$ requires the specification of the observational model: $D = \mathbf{I}X + \varepsilon$, where $\mathbf{I}$ is the interpolation operator, which establishes the relations between D and X. The interpolation is required since these fields are represented on different grids. The errors in the data are introduced as ε. Under the assumption that the errors in D are uncorrelated and the statistics is Gaussian, the probability density $p(D \mid X)$ (for a given X) can be expressed in terms of the data error statistics:

$$-\log p(D \mid X) = -\log p(\varepsilon) = -\log p(D - \mathbf{I}X) = (\mathbf{I}X - D)^T \mathbf{W_D} (\mathbf{I}X - D) \tag{A.3}$$

In (A.3), $\mathbf{W_D}$ is the inverse of the diagonal data error covariance matrix. For the Gaussian statistics of X, the cost function takes the following form:

$$J(X) = (\mathbf{I}X - D)^T \mathbf{W_D} (\mathbf{I}X - D) + (X - X_{REF})^T \mathbf{W_X} (X - X_{REF}) \tag{A.4}$$

In (A.4), the second term represents $-\log p(X)$, which is *a priori* statistics of the observed field X with a covariance matrix $C_{prior}(X)$ $\mathbf{W}_X^{-1}$ and the expectation value X_{REF}. Following the conventional approach (McIntosh, 1990), *a priori* correlations in the field X are approximated as follows

$$\begin{aligned}
&(X - X_{REF})^T \mathbf{W_X} (X - X_{REF}) = \\
&= (X - X_{REF})^T \mathbf{W_{REF}} (X - X_{REF}) - (\nabla^2 X)^T \mathbf{W_{SM}} (\nabla^2 X) - \\
&+ (\nabla H \times \nabla X)^T \mathbf{W_{BOT}} (\nabla H \times \nabla X).
\end{aligned} \tag{A.5}$$

In (A.5), $\mathbf{W}_{REF}$, $\mathbf{W}_{SM}$, $\mathbf{W}_{BOT}$ and are the diagonal weight matrices, and H is the bottom topography on the model grid. Finally, the optimal field X_{OPT} is obtained as a solution of the minimization of the cost function in the following form

$$\begin{aligned}
J(X) &= (\mathbf{I}X - D)^T \mathbf{W_D} (\mathbf{I}X - D) + (X - X_{REF})^T \mathbf{W_{REF}} (X - X_{REF}) + \\
&+ (\nabla^2 X)^T \mathbf{W_{SM}} (\nabla^2 X) + (\nabla H \times \nabla X)^T \mathbf{W_{BOT}} (\nabla H \times \nabla X)
\end{aligned} \tag{A.6}$$

The cost function $J(X)$ is a sum of the four terms in the right hand side of (A.6). The first term forces the algorithm to build the field that is close to the observations in the data locations. The second and the third terms in (A.6) take into account the correlations in the observed field X. The weight matrix $\mathbf{W}_{REF}$ in the second term of (A.6) is a diagonal matrix of the inverse variances of the reference field X_{REF}. ∇^2 is the approximation of the Laplace operator. The correlations between the bottom topography and the observed field X are imposed by adding the fourth term into (A.6). Though the value of the forth term is small, it is useful in the areas of a large bottom gradient, such as ship channels or barrier islands.

Numerical Procedure

The weights of the cost function (A.6) are estimated as follows

- $\mathbf{W}_{REF} = \left(\overline{(D - X_{REF})^2}\right)^{-1} = \mathrm{var}(D)^{-1}$, where $\mathrm{var}(D)^{-1}$ is a reciprocal of the data variances
- $\mathbf{W}_D = \left(10^{-2} \cdot \mathrm{var}(D)\right)^{-1}$
- $\mathbf{W}_{SM} = \mathrm{var}(D)^{-1} \cdot d^4$, where d is a characteristic distance between the data points
- $\mathbf{W}_{BOT} = (\mathrm{var}(\nabla H)\mathrm{var}(D))^{-1} \cdot d^2$, where H is the ECOM bottom topography

The Conjugate Gradient (Fletcher and Reeves, 1964) descent method is used to minimize the cost function (A.6). The optimal estimation of the mean temperature and salinity fields are computed at the ECOM horizontal grid ($N_x = 165 \times N_y$ grid points).

Appendix B
Variational interpolation error

The conventional way to estimate the posterior error covariance of the optimal solution is to compute the inverse of the Hessian matrix associated with the cost function:

$$C_{posterior}(X) = \left(\frac{\partial^2 J}{\partial X^2}\right)^{-1} \tag{B.1}$$

Since the dimension of the problem is relatively large (dim(X) ~ 10^6), we utilize a simplified approach to compute $C_{posterior}$. This approach is based on the linearity of the variational interpolation procedure:

$$X_{OPT} = L_1(D) + L_2(X_{REF}) = \sum_{i=1}^{N_D} L_{1i}(D_i) + \sum_{k=1}^{N_M} L_{2k}(X_{REF\,k}) \tag{B.2}$$

N_D in (B.2) is a number of the data points, $N_M = N_X \times N_Y$ is a number of the grid points in the field X, L_1 and L_2 are linear operators. By definition

$$\begin{aligned} C_{posterior}(X_{OPT}) &= L_1 C(D) L_1^T + L_2 C(X_{REF}) L_2^T = \\ &= \left(L_1 C(D)^{1/2}\right)\left(L_1 C(D)^{1/2}\right)^T + \left(L_2 C(X_{REF})^{1/2}\right)\left(L_2 C(X_{REF})^{1/2}\right)^T \end{aligned} \tag{B.3}$$

The data covariance matrix, $\boldsymbol{X}(D)$ is defined as

$$C(D) = \mathbf{W_D^{-1}} \tag{B.4}$$

Consequently,

$$C(D)^{1/2} = \sigma_D E, \tag{B.5}$$

where E is a unit matrix and σ_D is the standard deviation of the data error. As previously mentioned, σ_D was estimated as 1°C for temperature, and 2 ppt for salinity for this survey (Vinogradov et al., 2004). The covariance matrix of the reference field is defined as

$$C(X_{REF})^{1/2} = \sigma_{REF} E, \tag{B.6}$$

In (B.6), the standard deviation of the reference field error, σ_{REF}, was estimated as 7 – 9 ° C for temperature and 7 – 10 ppt for salinity (Vinogradov et al., 2004).

To estimate the terms $L_1C(D)^{1/2}$ and $L_2C(X_{REF})^{1/2}$ in (B.3), the variational interpolation technique is applied to a special kind of data and reference field. In order to estimate the term $L_1C(D)^{1/2}$, the technique is applied to the data, $D^* = \sigma_D$ and a zero reference field, $X^*_{REF} = 0$. To estimate the term $L_2C(X_{REF})^{1/2}$, the technique is applied to a reference field, $X^* = \sigma_{REF}$, and zero data, $D^* = 0$. Since we are interested in the error variance of the optimal field X_{OPT}, we discard the correlations in (B.3) and approximate var(X_{OPT})as:

$$\mathrm{var}_k(X_{OPT}) \approx \left[diag_k\left(L_1 C(D)^{1/2}\right)\right]^2 + \left[diag_k\left(L_2 C(X_{REF})^{1/2}\right)\right]^2,\ k = \ldots N_M \tag{B.7}$$

References

Ahsan, Q., A. F. Blumberg, H. Li, and J. Blaha. 2002. The Calibration/validation of a Mississippi Sound/Bight model. Proceedings of the MTS/IEEE Oceans 2002, Conference & Exhibition. 2:823-833.

Allen, J. S., P. A. Newberger, and J. Federiuk. 1995. Upwelling circulation on the Oregon continental shelf. J Phys Oceanogr. 25:1843-1866.

Asper V., J. P. Blaha, C. Szczechowki, C. Cumbeee, R. Williams, S. Lohrenz, D. Redaljie, and A.-P. Diercks. 2001. The Northern Gulf of Mexico Littoral Initiative (NGLI): a collaborative modeling, monitoring, and research effort. J Miss Acad Sci. 46(1):60.

Blumberg, A. F. and D. M. Goodrich. 1990. Modeling of wind-Induced destratification in Chesapeake Bay. Estuaries. 13:1236-1249.

Blumberg, A. F., Q. Ahsan, H. Li, and J. Blaha. 2002. An operational forecast modeling system for the Mississippi Sound/Bight. Proceedings of the MTS/IEEE Oceans 2002, Conference & Exhibition. 2:816-822.

Brooks, D. A. 1984. Current and hydrographic variability in the northwestern Gulf of Mexico. J Geophys Res. 89:8022-8032.
Chen, C. and R. C. Beardsley. 2002. Cross-frontal water exchange on Georges Bank: some results from an U.S. GLOBEC/Georges Bank program model study. J Oceanogr. 58:403-420.

Chen, C., R.C. Beardsley, and R. Limeburner. 1995. A numerical study of stratified tidal rectification over finite-amplitude banks. Part II: Georges Bank, J Phys Oceanogr. 25:2111-2128.

Chu, P. C., S. H. Lu and Y. C. Chen. 2001. Evaluation of the Princeton Ocean Model using South China Sea Monsoon Experiment (SCSMEX) data. J Atmos Ocean Tech. 18:1521-1539.

Fletcher, R. and C. M. Reeves. 1964. Function minimization by conjugate gradients. Computer Journal. 7:149-154.

Fong, D. A. and W. R. Geyer. 2001. Response of a river plume during upwelling favorable wind event. J Geophys Res. 106:1067-1084.

Fox, D.N., W.J. Teague and C.N. Barron. 2001. The Modular Ocean Data Assimilation System (MODAS), J Atmos Ocean Tech. 19:240-252.

Frigo, M. and S. G. Johnson. 1998. FFTW: An Adaptive Software Architecture for the FFT. Proceedings of the International Conference on Acoustics, Speech, and Signal Processing. 3:1381-1384.

Gerdes, R. 1993. A primitive equation ocean circulation model using a general vertical coordinate transformation. 1. Description and testing of the model. J Geophys Res. 98:14,683-14,701.

Hadivogel, D. B. and A. Beckmann. 1997. Numerical modeling of the coastal ocean. In: The Sea, K. H. Brink and A. R. Robinson, eds., 10, 457 – 482. New York: Wiley.

Hodur, R. M. 1997. The Naval Research Laboratory's Coupled Ocean/Atmosphere Mesoscale Prediction System (COAMPS). Mon Wea Rev. 125:1414-1430.

HydroQual. 2002. A Primer for ECOMSED. Version 1.3. 188 pp.

Keen, T. R., 2002. Waves and currents during a winter cold front in the Mississippi Bight, Gulf of Mexico: Implication for barrier island erosions. J. Coastal Res., 18, 622 – 636.

Keen, T. R. and S. E. Allen. 2000. The generation of internal waves on the continental shelf by Hurricane Andrew. J Geophys Res. 105:26,203-26,224.

Kelly, F. J. 1991. Physical oceanography/water mass characterization. Chapter 10 in: Mississippi-Alabama Continental Shelf Ecosystem Study: Data Summary and Synthesis. Volume II, Technical Narrative. J. M. Brooks, ed., Technical Rpt. OCS Study/ MMS 91-0063, U. S. Dept. of the Interior, Minerals Management Service, New Orleans, La., 10-1-10-151.

Kjerfve, B. 1983. Analysis and synthesis of oceanic conditions in Mississippi Sound, April Thru October 1980. Final Report to U.S. Army Engineer District, Mobile, Alabama. March 1983.

Klinck, J. M. 1995. Circulation near submarine canyons: A modeling study. J Geophys Res. 101:1211-1233.

McIntosh, P.C. 1990. Oceanic data interpolation: objective analysis and splines. J Geophys Res. 95:13, 529-13, 541.

Mellor, G. L. and T. Yamada. 1982. Development of turbulence closure model for geophysical fluid problems, Rev Geophys. 20:851-875.

Schroeder, W. W., S.P. Dinnel, W. J. Wisaman Jr. and W. J. Merrell Jr. 1987. Circulation patterns inferred from the mvement of detached bouys in the eastern Gulf of Mexico. Cont Shelf Res. 7:883-894.

Schroeder, W. W. and W. J. Wiseman Jr. 1999. Geology and hydrodynamics of Gulf of Mexico Estuaries. In: Biochemistry of Gulf of Mexico Estuaries, T. S. Bianchi, J. R. Pennock, R. R. Twilley, eds., 1 – 28. John Wiley & Sons, Inc.

Smagorinsky, J. S. 1963. General circulation experiments with the primitive equations. I. The basic experiment. Mon Weather Rev. 91:99-164.

Smolarkiewicz, P. K. and W. W. Grabowski. 1990. The multidimensional positive definite advection transport algorithm. J Comput Phys. 86:355-375.

Teng, C. C. 2003. Oceanographic data analysis. Notes for MAR 665, Stennis Space Center, MS.

Vinogradov, S. and N. Vinogradova. 2003. Northern Gulf of Mexico Temperature and Salinity Variability and ECOM Assessment Based on the Northern Gulf of Mexico (NGLI) Conductivity-Temperature-Depth (CTD) Data. Dept. of Mar. Sci. Final Report 2003-11., the Univ. of Southern Miss, Stennis Space Center, MS

Vinogradov, S., N. Vinogradova, V. Kamenkovich, and D. Nechaev. 2004. Temperature and salinity variability in the Mississippi Bight. MTS Journal, 38(1):52-60.